Transient Damage Spreading and Anomalous Scaling in Mortar Crack Surfaces

S. Morel,[1] D. Bonamy,[2] L. Ponson,[3] E. Bouchaud, [4]

[1] *Université Bordeaux 1, US2B (UMR5103), 351 cours de la Libération, 33405 Talence Cedex, France*

[2] *C.E.A.-Saclay, DSM/IRAMIS/SPCSI, 91191 Gif-Sur-Yvette Cedex, France*

[3] *California Institute of Technology, Division of Engineering and Applied Science, Pasadena, CA 91125, USA*

[4] *C.E.A.-Saclay, DSM/IRAMIS/SPEC, Groupe Instabilités et Turbulence, Orme des Merisiers, 91191 Gif-Sur-Yvette Cedex, France*

1. Introduction

Since the pioneering work of Mandelbrot et al [1], the statistical characterization of fracture surfaces is nowadays a very active field of research. The fracture surfaces of various materials show surprising scaling properties (see [2-3] for reviews) and especially self-affine scaling invariance over a wide range of length scales. Indeed, the fracture surfaces obtained in materials as different as metallic alloys [4-7], ceramics [8-9], glass [10-11], quasi-crystals [12-13], rocks [14-15], mortar [16-17], sea ice [18], and wood [19-20] exhibit self-affine scaling properties characterized by a local roughness exponent $\zeta \approx 0.8$ and this in spite of huge differences in the fracture mechanisms. It was therefore suggested that this local roughness exponent ζ, measured along the direction of crack front, might have a universal value [21], i.e., a value independent of the fracture mode and of the material.

However, quite recently, significantly different values of the local roughness exponent ζ have been measured due to the anisotropy and the heterogeneity of the material structure [7,21-23], the kinetics of crack growth [24] or the possible multifractal character of the crack surfaces [25]. On the other hand, fracture surfaces were shown to exhibit *anisotropic* scaling morphological features, characterized by two different roughness exponents whether observed along the direction of crack front or crack growth [10,12-13]. This anisotropic scaling was shown to take a universal specific form independent of the considered material, the failure mode and the crack growth velocity [12-13]. Finally, recent experiments in sandstone [26-27], artificial rock [28] and granular packing of sintered glass beads [11,29], which are materials exhibiting a brittle failure, have shown self-affine scaling properties, especially at large length scales, characterized by a roughness exponent measured along the direction of crack front closer to 0.4-0.5. These latter experimental results deserve some more thinking especially since the measured roughness indexes (0.4-0.5) are significantly smaller than 0.8 and hence they suggest the existence of a *second* universality class for failure problems.

A possible interpretation of both universality classes was proposed recently by Bonamy et al. [11]. It was indeed reported that 0.8 roughness exponent was

measured in materials where surfaces are observed at length scales *below* the size of the Process Zone (PZ) while the 0.4 roughness exponent is estimated at length scales *above* this PZ size. Such an interpretation is funded on recent results obtained from two distinctive models. First, Bonamy et al. [11] have derived a model from Linear Elastic Fracture-Mechanics (LEFM) that predicts 0.4 self-affine fracture surfaces for perfectly brittle materials, i.e., according to LEFM, in the absence of any damage and/or plastic deformations. Thus, the 0.4 roughness exponent could reflect the roughness of fracture surfaces at length scales where the material can be approximated as a linear elastic medium and, as a consequence, at length scales above the PZ size. Second, using a paradigm of the mode I fracture model (quasistatic fuse model), Hansen and Schmittbuhl [30] have suggested that the universality of 0.8 roughness exponent could be due to a fracture propagation being a universal damage coalescence process described by a stress-weighted percolation phenomenon in a self-generated quadratic damage gradient. In this sense, the 0.8 roughness exponent could reflect the roughness of fracture surfaces at length scales below the PZ size, i.e., where such a damage percolation process can take place. However, the two regimes had never been observed on the same material and, all the more so, on the same fracture surface. It is the central point of this study to show that both regimes can be observed on a mortar fracture surface.

2. Experiment

The studied fracture surface is obtained from a mortar notched beam subjected to four points bending leading to a mode I failure [16-17]. The length of the beam is 1400 mm and its height and thickness are both equal to 140 mm. The initial notch is performed with a steel sheet (thickness 0.4 mm) pulled out when the mortar is 24 hours old. The notch length is fixed to 70 mm, which corresponds to half the beam height (Fig. 1).

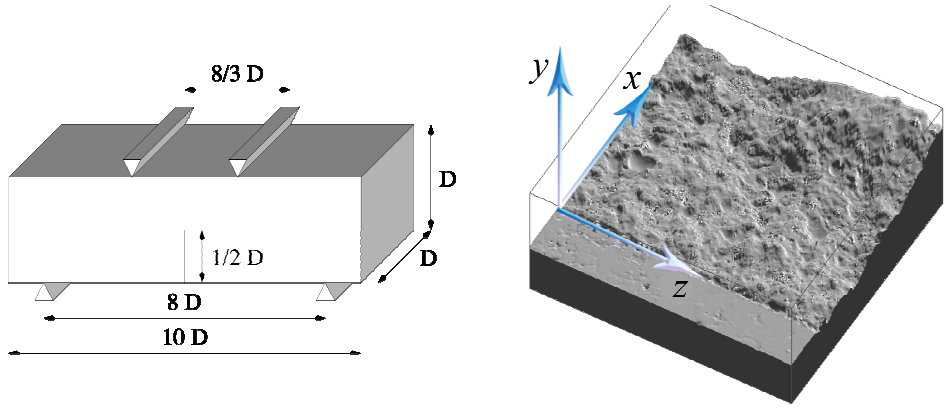

Figure 1. Left :Geometry of the notched bending specimen (D = 140 mm). Right : Topography of the mortar crack surface . The axis $\vec{x}$, $\vec{y}$ and $\vec{z}$ are parallel to the propagation, loading and crack front directions respectively

The mortar is constituted by a sand for which the grain size ranges between 0.1 mm and 1.8 mm, and by a high strength Portland cement. On the other hand, the

specimen geometry and test set-up lead to a mode I stable crack growth for the first 10-15 mm of the crack. Within this range of crack lengths, fracture can be considered as quasi-static.
The topographies of the fracture surfaces have been recorded using an optical profilometer. In all the following, the reference frame $(\vec{x},\vec{y},\vec{z})$ is chosen so that $\vec{x}$, $\vec{y}$ and $\vec{z}$ are parallel to the propagation, loading and crack front directions respectively (i.e., the average plane of the crack surface corresponds to the $(\vec{x},\vec{z})$ plane). The topographic maps are built up with 300 profiles of 4096 points parallel to the initial notch ($\vec{z}$ direction). The sampling step Δz along profiles is 20 µm while the distance between two successive profiles Δx is fixed to 50 µm. The first profile ($x = 0$) is sampled in the immediate vicinity of the initial straight notch tip and so corresponds to a quasi zero roughness. As the distance x to the initial notch increases, the magnitude of the roughness develops up to 7 mm (Fig.1). The lateral precision (i.e., along the x and z directions) is 2 µm while the vertical accuracy (i.e., along the y axis), estimated from the height differences between two successive profiles along the same line, is approximately 5 µm.

1.1. Local roughness regimes.
The roughness of the crack profiles and especially the development of this roughness with respect to the distance x from the initial notch can be estimated through the root mean square (RMS) $\Delta h(l,x)$ of the heights $h(z_i,x)_{1<i<N\_l}$ inside a window of size l [m] along the z-axis (N_l corresponds to the number of points in the window of size l) and averaged over all possible origins j of the window belonging to the profile:

$$\Delta h(l,x) = \left\langle \frac{1}{N_l}\sum_{i=1}^{N_l} h(z_i,x)^2 - \left[\frac{1}{N_l}\sum_{i=1}^{N_l} h(z_i,x)\right]^2 \right\rangle_j^{1/2} . \qquad (1)$$

Figure 2 corresponds to a log-log plot of the variations of the RMS roughness Δh with respect to the window size l for two distinct profiles; the first profile, corresponding to $x = x_1$, is close to the initial notch while the second one, corresponding to $x = x_2$, is far from the notch. On each profile, two distinct behaviors corresponding to two power laws can be observed. The first power law observed at small length scales is characterized by a roughness exponent $\zeta = 0.79$, while the second power law, observed at large length scales, is characterized by a different roughness index $\zeta_e = 0.41$. Note that, both roughness indexes ($\zeta = 0.79$ and $\zeta_e = 0.41$), observed on the same crack profile, are consistent with the two universality classes of the roughness (related to the exponents 0.8 and 0.4) proposed in [11]. On the other hand, if one defines as ξ the abscissa of the intersection between the fits of both power laws, this crossover length is found to increase with the distance x to the initial notch, $\xi(x_1) < \xi(x_2)$, as shown in Fig. 2. Note that, the increasing of the distance x from the initial notch, which leads to a corresponding increase of the crossover length scale $\xi(x)$, favors the small scales regime related to the roughness index 0.8, to the detriment of the large scales regime associated to the index 0.4.

1.2. Roughening of the crack surface: anomalous scaling.

As can be seen in Figure 2, the magnitude of the RMS roughness of the profile at position $x = x_2$ is larger than the one of the profile at position $x = x_1$ and this whatever the considered length scale l. This global vertical shift of the $\Delta h(l,x)$ curves with respect to the distance x from the initial notch is well known to be symptomatic of an anomalous scaling [16-17,20-21,32-33]. Nevertheless, in the present case, the original anomalous scaling proposed in literature [20-21,32-33] needs to be modified in order to take into account the existence of both the local roughness regimes characterized by the indices $\zeta \approx 0.8$ and $\zeta_e \approx 0.4$ (as shown Fig. 2). Thus, let us assume that the crossover length scale ξ between these two regimes scales with the distance x from the initial notch, as a power law characterized by the dynamic exponent z_x: $\xi(x) \sim x^{1/z_x}$. On this basis, the original anomalous scaling can be modified in the following way:

$$\Delta h(l,x) \sim \begin{cases} l^{\zeta} x^{(\zeta_g - \zeta)/z_x} & \text{if } l << x^{1/z_x}, \\ l^{\zeta_e} x^{(\zeta_g - \zeta_e)/z_x} & \text{if } l >> x^{1/z_x}. \end{cases} \qquad (2)$$

Note that ζ_g is called as global roughness exponent and is considered as different from and independent on both local roughness indexes ζ and ζ_e.

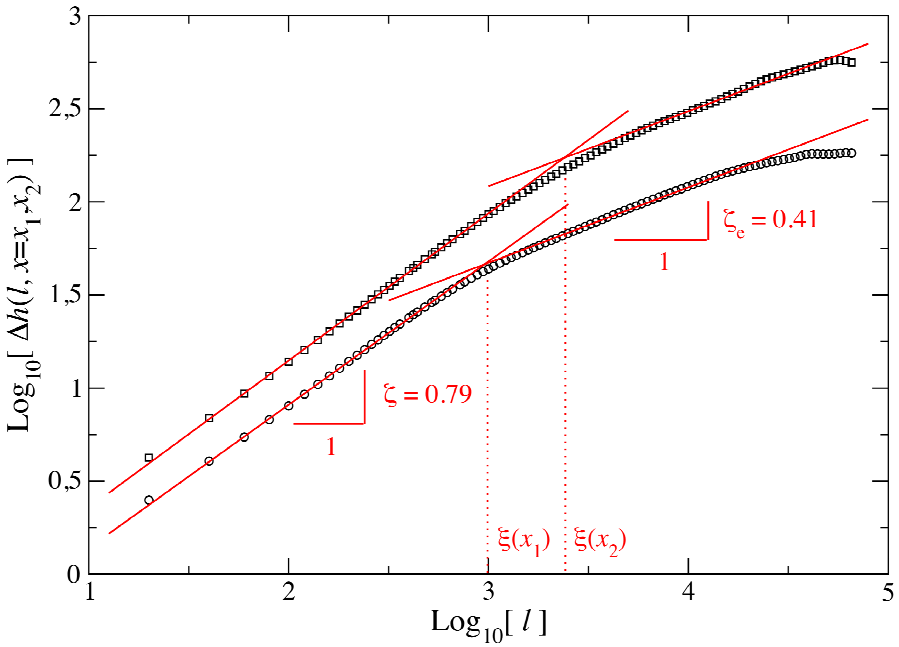

Figure 2. RMS roughness $\Delta h(l)$ with respect to the window size l for two profiles located at the beginning ($x = x_1$, circles) and at the end ($x = x_2$, squares) of the transient roughening domain. The slopes of both straight lines give estimates of the local roughness exponents $\zeta = 0.79$ (for $l << \xi$) and $\zeta_e = 0.41$ (for $l >> \xi$). All length scales are given in µm.

Thus, if one considers a profile at a given position x, the RMS roughness is expected to scale, according to Eq.(2), as $\Delta h(l << \xi, x = cte) \sim l^{\zeta}$ for length scales

$l << \xi(x)$ while, for length scales $l >> \xi(x)$, the roughness scales as $\Delta h(l >> \xi, x = cte) \sim l^{\zeta_e}$ which is in agreement with the scaling observed in Fig. 2. On the other hand, if the roughness development is observed with respect to the distance x from the initial notch, the roughness estimated for a given small length scale, i.e., $l = cte$ and $l << \xi(x)$, scales as $\Delta h(l = cte, x) \sim x^{(\zeta_g - \zeta)/z_x}$ while, the roughness for a given large length scale, i.e., $l = cte$ and $l >> \xi(x)$, is expected to scale as $\Delta h(l = cte, x) \sim x^{(\zeta_g - \zeta_e)/z_x}$.

The latter roughening expected at small and large length scales from Eq.(2) can be observed in plotting the RMS roughness with respect to the distance x as shown in Figure 3. Note that in Fig. 3, only some window sizes ranging from l = 20 µm to 60 mm are kept, for the sake of clarity. The RMS roughness Δh grows as a function x from approximately zero for profiles close to the initial straight notch.

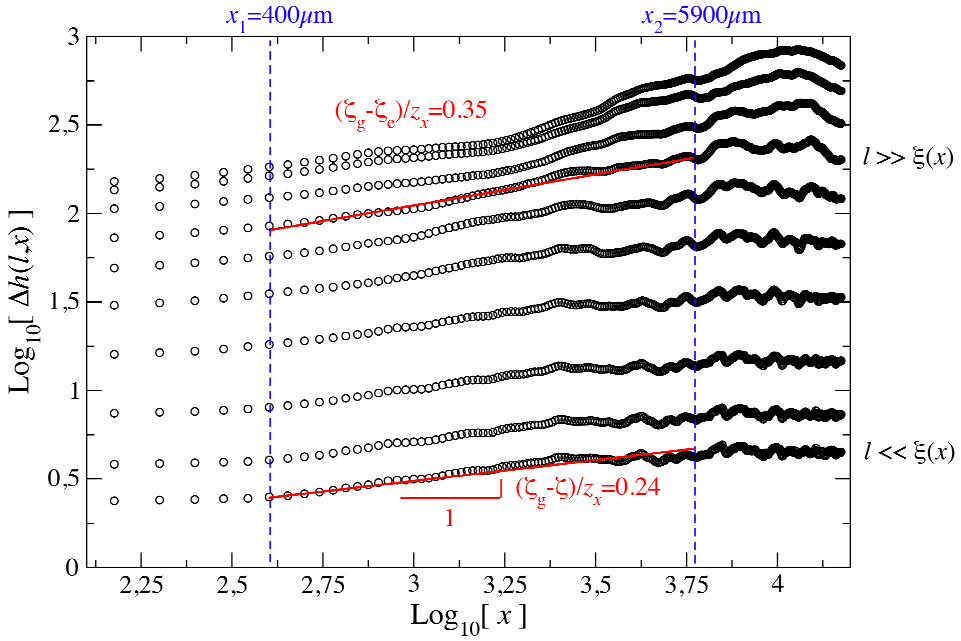

Figure 3. Log-log plot of the RMS roughness $\Delta h(l,x)$ with respect to the distance x from the initial notch. The roughness growth domain corresponds to the part between the position x_1 and x_2. According to Eq.(2), the lower straight line corresponds to the fit of the roughness growth observed for a small length scale, i.e., $l << \xi(x)$, and its slope (0.24) is expected to give an estimate of the scaling exponent $(\zeta_g - \zeta)/z_x$ while, the upper line is expected to correspond to the roughness growth for a large length scale $l >> \xi(x)$ and its slope (0.35) leads to the estimate of the scaling exponent $(\zeta_g - \zeta_e)/z_x$.

In Fig. 3, the roughness development is essentially observed for x values ranging between x_1 and x_2 which correspond to the positions of the profiles plotted in Fig.

2. For distances $x < x_1 \cong 400\mu m$, the roughness magnitude remains approximately whatever the position x. This phenomenon can be attributed to the non-zero thickness of the initial notch (0.4 mm as previously mentioned) which leads to a corresponding non-zero roughness at the onset of crack propagation. On the other hand, distances $x > x_2 \cong 5.9$ mm, it can be observed in Fig. 3 that the roughness magnitude saturates for a wide range of length scales l. Nevertheless, for the largest length scales l, the roughness exhibits fluctuations which are doubtlessly due to a slight macroscopic warping of the fracture surface. Within the growing zone, i.e., for distances $x_1 < x < x_2$, it can be observed from Fig. 3 that the roughness growth is different if considered for length scales smaller or greater than the crossover length scales $\xi(x)$. Note that such different roughness growths can be also observed in Fig.2 from the vertical shifts of the RMS roughness observed for position x_1 and x_2 which are different if observed at length scales $l << \xi(x)$ and $l >> \xi(x)$.

On the other hand, the more efficient way to estimate the global roughness index ζ_g and the dynamic exponent z_x consists to introduce the scaling function describing the scaling behavior $\Delta h(l,x)$ expected from Eq.(2). Thus, from the *modified* anomalous scaling defined in Eq.(2), let us define the scaling function $g_m(u)$ as $g_m\left(l/x^{1/z_x}\right) = \Delta h(l,x)/l^{\zeta_g}$ and hence, the scaling function $g_m(u)$ is expected to scale as

$$g_m(u) \sim \begin{cases} u^{-(\zeta_g - \zeta)} & \text{if } u << 1, \\ u^{-(\zeta_g - \zeta_e)} & \text{if } u >> 1. \end{cases} \qquad (3)$$

where $u = l/x^{1/z_x}$. The method used to estimate the global roughness index ζ_g and the dynamic exponent z_x consists to compute the experimental values $g_m(u)$ for various values of ζ_g and z_x while the values of the local roughness exponents are kept equal to the previous estimate (i.e., $\zeta = 0.79$ and $\zeta_e = 0.41$ as shown in Fig. 2) and this for all profiles corresponding to the roughness growth domain (i.e., corresponding to positions ranging between x_1 and x_2). The best data collapse, which corresponds to the least scattering of the experimental values $g_m(u)$, is obtained for the scaling exponent values $\zeta_g = 1.60 \pm 0.10$ and $z_x = 3.4 \pm 0.20$ as shown in Figure 4. Note that the global roughness index ζ_g and the dynamic exponent ζ_g and z_x have distinct influences on the date collapse. Indeed, the dynamic exponent z_x acts on the scattering of the experimental data along the abscissa axis while the global roughness index ζ_g has an influence on the scattering along the ordinates axis (Fig. 4). On the other hand, the optimal values of the scaling exponents obtained from the scaling function ($\zeta_g = 1.60 \pm 0.10$ and $z_x = 3.4 \pm 0.2$) are in agreement with the corresponding values which can be estimated from the slopes of the straight lines plotted in Fig. 3. Indeed, according to Eq.(2), the slope of the lower line (0.24) which corresponds to the fit of roughness estimated for a small length scale, i.e., $l << \xi(x)$, gives an estimate of the scaling exponent $(\zeta_g - \zeta)/z_x$ while the one of the upper line (0.35) which is related to the roughness observed for a large length scale, i.e., $l >> \xi(x)$ leads to the estimate of the scaling exponent $(\zeta_g - \zeta_e)/z_x$.

3. Discussion

From the roughness analysis of a mortar crack surface, it has been shown that both roughness regimes characterized by the local exponents $\zeta \approx 0.8$ and $\zeta_e \approx 0.4$ can co-exist on the same fracture surface and especially along the same crack profile. Moreover, both local roughness regimes have been observed in the presence of anomalous roughening and this has led to modify the original anomalous scaling [32]. The remarkable collapse of the 110 profiles located in the growing zone of roughness (Fig. 4) is in fair agreement with the modified anomalous scaling proposed in Eq.(2). On the other hand, the two local roughness exponents $\zeta \approx 0.8$ and $\zeta_e \approx 0.4$ are observed at small and large length scales respectively. These observations are consistent with the picture proposed by Bonamy et al [11] which suggests that the 0.4 roughness index should be observed at length scales where the material can be approximated as a linear elastic medium, i.e., et length scales larger than the PZ size, while the 0.8 exponent reflects the presence of damage at length scales smaller than the size of the PZ.

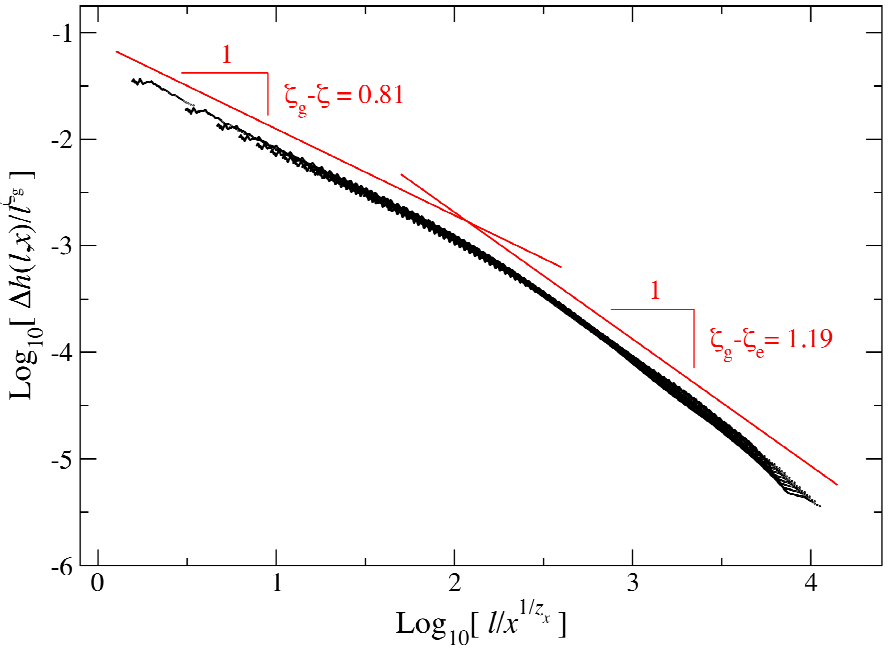

Figure 4. Modified anomalous scaling function $g_m(u)$ defined in Eq. (3). The best data collapse of the 110 profiles corresponding to positions ranging between x_1 = 400 µm and x_2 = 5.9 mm (roughness growth domain) is obtained for the scaling exponent values: $\zeta = 0.79$, $\zeta_e = 0.41$, $\zeta_g = 1.60 \pm 0.10$ and $z_x = 3.4 \pm 0.2$.

According to this scenario, the crossover length scale ξ is expected to set by the *PZ size* or, more exactly, by a correlation length of the PZ in the direction perpendicular to the crack propagation one. This correlation length could be

linked to a correlated gradient percolation process in PZ as suggested by Hansen and Schmittbuhl [30]. On the other hand, the increase of the correlation length ξ within the transient roughening regime with the distance x from the initial straight notch (i.e., for distances $x_1 < x < x_2$) is then fully consistent with the quasibrittle fracture behavior of mortar, characterized by a transient initial regime reflecting the increase in size of the microcracked PZ and/or the increase in microcracks density in PZ before reaching its critical and steady value. In this sense, the extension of the transient roughening regime given by the position x_2 could reflect the trace of the PZ development (attached to the initial notch tip) before the propagation of the main crack with its critical PZ. Thus, the maximum crossover length scale $\xi_{max} = \xi(x_2)$\$ as well as the extension x_2 of the transient roughening regime could provide post mortem estimates of length scales linked to the critical PZ in the directions perpendicular and parallel to the crack propagation direction. Note that these values of the length scales expected to be linked to the PZ, i.e., ξ_{max} = 2.3 mm and x_2 = 5.9 mm, are of the same order of magnitude as the estimates of the equivalent LEFM length of PZ usually obtained in mortar [34]. Note also that ξ_{max} = 2.3 mm is slightly larger than the largest grains of sand (1.8 mm).

On the other hand, the dynamic exponent z_x could characterize the evolution in size of the microcracked PZ and/or the increase in microcracks density in PZ with respect to the distance x from the initial notch through the evolution of the correlation length $\xi(x) \sim x^{1/z_x}$. In the same way, estimated at the crossover length scale $l = \xi$ according to Eq.(2), the roughness $\Delta h(l = \xi, x) \sim \xi^{\zeta_g}$ could provide an estimate of the maximum height fluctuations in the PZ, and, indirectly, of the magnitude of the toughness fluctuations/microcracks density inside this zone. Therefore, the global roughness exponent ζ_g could be the signature of the transient damage spreading and this is why it could be material dependent as previously proposed in [16,17,20,21] contrary to both local roughness indices ζ and ζ_e which should be considered as universal.

4. Conclusion

On the basis of the results presented in this paper, one can now reinterpret the values of the roughness exponents (measured for fracture profiles parallel to the direction of crack front) reported in the literature [4,5,7-21,26-29] for various materials:

(i) When the PZ size remains small with respect to the specimen size, as for brittle failure, the crossover length scale ξ is expected to be very small. In this case, the 0.8 roughness regime should be only observed for the smallest length scales (and hence, may be difficult to observed experimentally) while the 0.4 roughness regime is expected to take place over a wide range of length scales. This is the case of materials such sandstone [26,27], artificial rocks [28] and granular packing of sintered glass beads [29] for which the 0.4 roughness regime is well observed while the 0.8 roughness regime seems inexistent (or difficult to observe because only effective for the smallest length scales). Then, models derived from LEFM such as [11,35] should be able to capture the

morphology of fracture surfaces. In particular, such models can reproduce 0.4 roughness regimes in agreement with observations reported in [26-29]. Moreover, damage spreading within the process zone should be scarce in brittle failure, and one expects to observe a classical Family-Vicsek roughening [36] rather than an anomalous scaling [32,33].

(ii) When the process zone size becomes important as compared to the specimen size, as for quasi-brittle failure, one expects to observe a large crossover length scale ξ. In this case, the 0.8 roughness regime should take place over a wide range of length scales while the 0.4 roughness regime should be only observed for the largest length scales where it can be perturbed by a finite size effect making its observation difficult. Moreover, the quasi-brittle damage spreading from a straight notch (i.e., the increase of the microcracked PZ size and/or the increase in microcracks density within the PZ) is expected to lead to an anomalous scaling rather than a Family-Vicsek one, as reported for mortar [16] and wood [20]. Finally, the fact that the value of the roughness exponent is observed close to 0.8 in very different materials with various damage processes as e.g. plastic deformation, crack blunting, ductile cavity growth or microcracking is in agreement with the suggestion [30] of a universal correlated gradient percolation process (i.e., a process independent of the precise nature of the damage).

To test this scenario experimentally will represent interesting challenges for future investigations.

References.

[1] B.B. Mandelbrot, D.E. Passoja, and A.J. Paullay, Nature 308 (1984), 721.
[2] E. Bouchaud, J. Phys. Cond. Mat. 9 (1997), 4319.
[3] E. Bouchaud, Surf. Rev. Lett. 10 (2003), 73.
[4] E. Bouchaud, G. Lapasset and J. Planés, Europhys. Lett. 13 (1990), 73.
[5] R. H. Dauskardt, F. Haubensk and R. O. Ritchie, Acta Metall. Mater. 38 (1990), 143.
[6] A. Imre, T. Pajkossy and L. Nyikos, Acta Metall. Mater. 40 (1992), 1819.
[7] S. Morel, T. Lubet, J.-L. Pouchou and J.-M. Olive, Phys. Rev. Lett. 93 (2004), 065504.
[8] J. J. Mecholsky, D. E. Passoja and K. S. Feinberg-Ringel, J. Am. Ceram. Soc. 72 (1989), 60.
[9] K. J. Måløy, A. Hansen, E. L. Hinrichsen and S. Roux, Phys. Rev. Lett. 68 (1992), 213.
[10] L. Ponson, D. Bonamy, E. Bouchaud, Phys. Rev. Lett. 96 (2006), 035506.
[11] D. Bonamy, L. Ponson, S. Prades, E. Bouchaud and C. Guillot, Phys. Rev. Lett. 97 (2006), 135504.
[12] L. Ponson, D. Bonamy, L. Barbier, Phys. Rev. B 74 (2006), 184205. [13]
[13] L. Ponson, Ann. Phys. Fr. 32 (2007), 1.
[14] J. Schmittbuhl, F. Schmitt and C. Scholz, Geo. Res. 100 (1995), 5953.
[15] J. M. López and J. Schmittbuhl, Phys. Rev. E 57 (1998), 6405.
[16] G. Mourot, S. Morel, E. Bouchaud and G. Valentin, Phys. Rev. E 71 (2005), 016136.

[17] G. Mourot, S. Morel, E. Bouchaud and G. Valentin, Int. J. Fract. 140 (2006), 39.
[18] J. Weiss, Eng. Fract. Mech. 68 (2001), 1975.
[19] T. Engøy, K. J. Måløy, A. Hansen and S. Roux, Phys. Rev. Lett. 73 (1994), 834.
[20] S. Morel, J. Schmittbuhl, J. M. López and G. Valentin, Phys. Rev. E 58 (1998), 6999.
[21] S. Morel, G. Mourot and J. Schmittbuhl, Int. J. Fract. 121 (2003), 23.
[22] I. L. Menezes-Sobrinho, M. S. Couto and I. R. B. Ribeiro, Phys. Rev. E 71 (2005), 066121.
[23] A. S. Balankin, O. Susarrey and J. M. González, Phys. Rev. Lett. 90 (2003), 096101.
[24] N. Mallick, P.-P. Cortet, S. Santucci, S. G. Roux and L. Vanel, Phys. Rev. Lett. 98 (2007), 255502.
[25] E. Bouchbinder, I. Procaccia, S. Santucci and L. Vanel, Phys. Rev. Lett. 96 (2206), 055509.
[26] J. M. Boffa, C. Allain and J.-P. Hulin, Eur. Phys. J. AP. 2 (1998), 281.
[27] L. Ponson, H. Auradou, M. Pessel, V. Lazarus and J.-P. Hulin, Phys. Rev. E 76 (2007), 036108.
[28] E. Bouchbinder, I. Procaccia and S. Sela, Phys. Rev. Lett. 95 (2005), 255503.
[29] L. Ponson, H. Auradou, P. Vié and J.-P. Hulin, Phys. Rev. Lett. 97 (2006), 125501.
[30] A. Hansen and J. Schmittbuhl, Phys. Rev. Lett. 90 (2003), 045504.
[31] S. Morel, J. Schmittbuhl, E. Bouchaud and G. Valentin, Phys. Rev. Lett. 85 (2000), 1678.
[32] J.M. López and M.A. Rodríguez, Phys. Rev. E. 54 (1996), R2189.
[33] J. M. López, M. A. Rodríguez and R. Cuerno, Phys. Rev. E 56 (1997), 3993.
[34] Z.P. Bazant and Z. Li, J. Engng. Mech. 122 (1996), 458.
[35] S. Ramanathan, D. Ertas, and D. S. Fisher, Phys. Rev. Lett. 79 (1997), 873.
[36] F. Family and T. Vicsek, Dynamics of fractal surfaces, World Scientific, Singapore, 1991.